

Serial No.: 09/553,993  
Filed: April 20, 2000

### CLEAN VERSION CLAIMS

We claim:

1. (Amended) A method of detecting a target nucleic acid sequence, said method comprising:
  - a) attaching a first adapter nucleic acid to a first target nucleic acid sequence to form a modified first target nucleic acid sequence;
  - b) contacting said modified first target nucleic acid sequence with an array comprising:
    - i) a substrate with a patterned surface comprising discrete sites; and
    - ii) a population of microspheres comprising at least a first subpopulation comprising a first nucleic acid capture probe which hybridizes to said first adapter nucleic acid, wherein said microspheres are distributed on said patterned surface at said discrete sites; and
  - c) detecting the presence of said modified first target nucleic acid sequence as an indication of the presence of said first target nucleic acid sequence.
2. (Amended) The method according to claim 1 further comprising:
  - a) attaching a second adapter nucleic acid to a second target nucleic acid sequence to form a modified second target nucleic acid sequence;
  - b) contacting said modified second target nucleic acid sequence with said array, wherein said population of microspheres comprises at least a second subpopulation comprising a second nucleic acid capture probe, which hybridizes to said second adapter nucleic acid; and
  - c) detecting the presence of said modified second target nucleic acid sequence as an indication of the presence of said second target nucleic acid sequence.
3. The method according to claim 1, wherein said attaching is by an amplification reaction.
4. The method according to claim 3, wherein said amplification reaction is the polymerase chain reaction (PCR).
5. The method according to claim 3, wherein said amplification reaction is the oligonucleotide ligation amplification reaction (OLA).
6. The method according to claim 1, wherein said attaching is by chemical synthesis.
7. The method according to claim 1, wherein said modified target nucleic acid sequence comprises a label.
8. The method according to claim 6, wherein said label is a fluorescent label.
9. The method according to claim 6, wherein said adapter nucleic acid is labeled.
10. The method according to claim 6, wherein said target nucleic acid sequence is labeled prior to said attaching.

**Serial No.:** 09/553,993  
**Filed:** April 20, 2000

11. The method according to claim 1, wherein said detecting is done by hybridizing a label probe to said modified target nucleic acid sequence.
12. The method according to claim 1, wherein said substrate is a fiber optic bundle.
13. The method according to claim 1, wherein said discrete sites comprise wells.
14. (Amended) A method of detecting a target nucleic acid sequence comprising:
  - a) hybridizing a first primer to a first portion of a target sequence, wherein said first primer further comprises an adapter sequence;
  - b) hybridizing a second primer to a second portion of said target sequence;
  - c) ligating said first and second primers together to form a modified primer;
  - d) contacting said adapter sequence of said modified primer with an array comprising:
    - i) a substrate with a surface comprising discrete sites; and
    - ii) a population of microspheres comprising at least a first subpopulation comprising a first nucleic acid capture probe, that hybridizes to said adapter sequence, wherein said microspheres are distributed on said surface; and
  - e) detecting the presence of said modified primer, to thereby detect said target nucleic acid sequence.

# Light-generated oligonucleotide arrays for rapid DNA sequence analysis

(sequencing by hybridization/combinatorial chemistry/DNA diagnostics)

ANN CAVIANI PEASE<sup>†</sup>, DENNIS SOLAS<sup>†</sup>, EDWARD J. SULLIVAN<sup>†</sup>, MAUREEN T. CRONIN<sup>‡</sup>,  
CHRISTOPHER P. HOLMES<sup>†</sup>, AND STEPHEN P. A. FODOR<sup>†‡</sup>

<sup>†</sup>Affymetrix, 3380 Central Expressway, Santa Clara, CA 95051; and <sup>‡</sup>Affymax, 4001 Miranda Avenue, Palo Alto, CA 94304

Communicated by Ronald W. Davis, January 4, 1994

**ABSTRACT** In many areas of molecular biology there is a need to rapidly extract and analyze genetic information; however, current technologies for DNA sequence analysis are slow and labor intensive. We report here how modern photolithographic techniques can be used to facilitate sequence analysis by generating miniaturized arrays of densely packed oligonucleotide probes. These probe arrays, or DNA chips, can then be applied to parallel DNA hybridization analysis, directly yielding sequence information. In a preliminary experiment, a  $1.28 \times 1.28$  cm array of 256 different octanucleotides was produced in 16 chemical reaction cycles, requiring 4 hr to complete. The hybridization pattern of fluorescently labeled oligonucleotide targets was then detected by epifluorescence microscopy. The fluorescence signals from complementary probes were 5–35 times stronger than those with single or double base-pair hybridization mismatches, demonstrating specificity in the identification of complementary sequences. This method should prove to be a powerful tool for rapid investigations in human genetics and diagnostics, pathogen detection, and DNA molecular recognition.

Conventional DNA sequencing technology is a laborious procedure requiring electrophoretic size separation of labeled DNA fragments. An alternative approach to *de novo* DNA sequencing, termed sequencing by hybridization (SBH), has been proposed (1–3). This method uses a set of short oligonucleotide probes of defined sequence to search for complementary sequences on a longer target strand of DNA. The hybridization pattern is then used to reconstruct the target DNA sequence. It is envisioned that hybridization analysis of large numbers of probes can be used to sequence long stretches of DNA. In more immediate applications of hybridization methodology, a small number of probes can be used to interrogate local DNA structure.

The strategy of SBH can be illustrated by the following example. A 12-mer target DNA sequence, AGCCTAGCTGAA, is mixed with a complete set of octanucleotide probes. If only perfect hybridization complementarity is considered, 5 of the 65,536 octamer probes—TCGGATCG, CGGATCGA, GGATCGAC, GATCGACT, and ATCGACTT—will hybridize to the target. Alignment of the overlapping sequences from the hybridizing probes reconstructs the complement of the original 12-mer target:

```
TCGGATCG
CGGATCGA
GGATCGAC
GATCGACT
ATCGACTT
TCGGATCGACTT
```

Hybridization methodology can be carried out by attaching target DNA to a surface. The target is then interrogated with a set of oligonucleotide probes, one at a time (4, 5). This approach can be implemented with well-established methods of immobilization and hybridization detection but involves a large number of manipulations. For example, to probe a sequence utilizing a full set of octanucleotides, tens of thousands of hybridization reactions must be performed.

Alternatively, SBH can be carried out by attaching probes to a surface in an array format where the identity of the probe at each site is known. The target DNA is then added to the array of probes. The hybridization pattern determined in a single experiment directly reveals the identity of all complementary probes. The testing of this SBH format has required the development of new technologies for the fabrication of oligonucleotide arrays (6, 7). Most recently, an oligonucleotide array of 256 octanucleotides was generated using a solution-channeling device to direct the oligonucleotide probe synthesis into  $3 \times 3$  mm sites (7). In this format, the resolution limit of approximately  $1 \times 1$  mm may ultimately limit the number of probes that one can synthesize on a substrate of a manageable size (7).

We report here a method by which light is used to direct the synthesis of oligonucleotide probes in high-density, miniaturized arrays. Photolabile 5'-protected *N*-acyl-deoxynucleoside phosphoramidites, surface linker chemistry, and versatile combinatorial synthesis strategies have been developed for this technology. A matrix of 256 spatially defined oligonucleotide probes was generated, and the ability to use the array to identify complementary sequences was demonstrated by hybridizing fluorescently labeled octanucleotides. The hybridization pattern demonstrates a high degree of base specificity and reveals the sequence of oligonucleotide targets.

## MATERIALS AND METHODS

The basic strategy for light-directed oligonucleotide synthesis (6) is outlined in Fig. 1. The surface of a solid support modified with photolabile protecting groups (X) is illuminated through a photolithographic mask, yielding reactive hydroxyl groups in the illuminated regions. A 3'-*O*-phosphoramidite-activated deoxynucleoside (protected at the 5'-hydroxyl with a photolabile group) is then presented to the surface and coupling occurs at sites that were exposed to light. Following capping, and oxidation, the substrate is rinsed and the surface is illuminated through a second mask, to expose additional hydroxyl groups for coupling. A second 5'-protected, 3'-*O*-phosphoramidite-activated deoxynucleoside is presented to the surface. The selective photodeprotection and coupling cycles are repeated until the desired set of products is

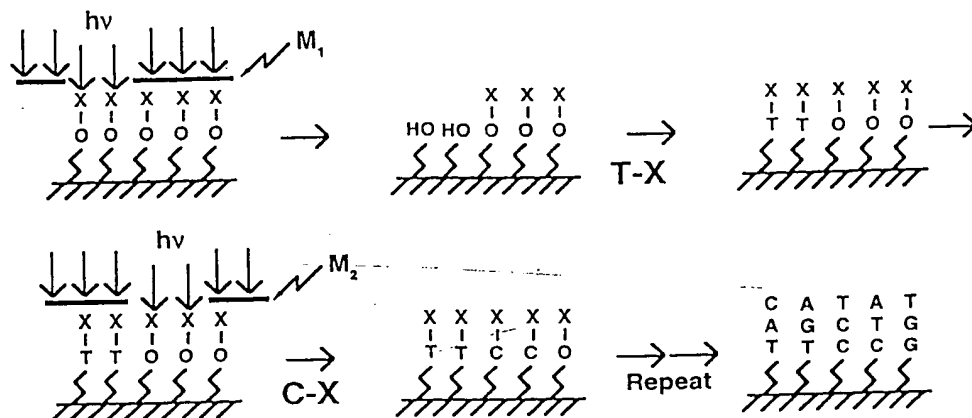


FIG. 1. Light-directed synthesis of oligonucleotides. A surface bearing photoprotected hydroxyls (X-O) is illuminated through a photolithographic mask (M<sub>1</sub>), generating free hydroxyl groups in the photodeprotected regions. The hydroxyl groups are then coupled to a deoxynucleoside phosphoramidite (5'-photoprotected). A new mask pattern (M<sub>2</sub>) is applied, and a second photoprotected phosphoramidite is coupled. Rounds of illumination and coupling are repeated until the desired set of products is obtained.

obtained. Since photolithography is used, the process can be miniaturized to generate high-density arrays of oligonucleotide probes. Furthermore, the sequence of the oligonucleotides at each site is known.

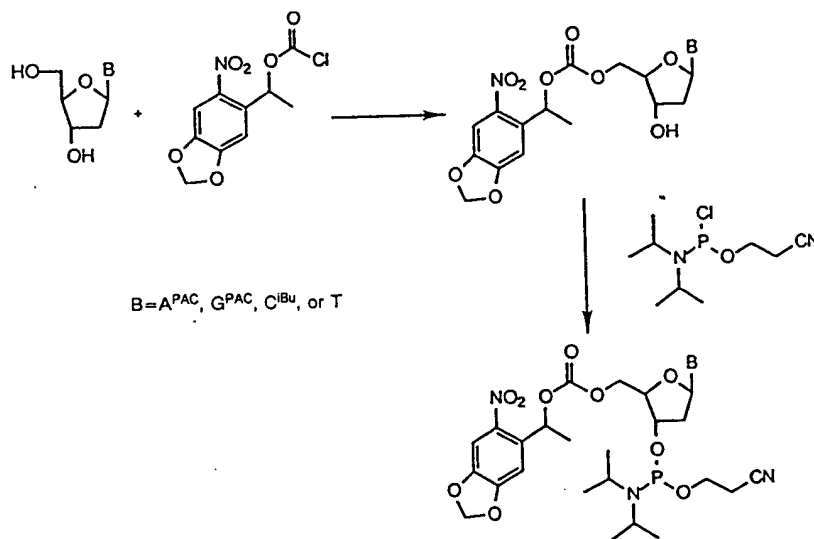
**5'-Photolabile *N*-Acyl-deoxynucleoside-3'-*O*-phosphoramidites.** Two factors enter into the design of photolabile 5'-hydroxyl protecting groups. Because the bases have strong  $\pi-\pi^*$  transitions in the 280-nm region, the deprotection wavelength should be longer than 280 nm to avoid undesirable nucleoside photochemistry. In addition, the photodeprotection rates of the four deoxynucleosides should be similar so that light will equally effect deprotection in different illuminated synthesis sites. To meet these criteria we have developed a set of 5'-*O*-( $\alpha$ -methyl-6-nitropiperonyloxycarbonyl)-*N*-acyl-2'-deoxynucleosides (MeNPoc-*N*-acyl-deoxynucleosides) and measured their photokinetic behavior.

The synthetic pathway for preparing 5'-*O*-( $\alpha$ -methyl-6-nitropiperonyloxycarbonyl)-*N*-acyl-2'-deoxynucleoside phosphoramidites (MeNPoc-*N*-acyl-2'-deoxynucleoside phosphoramidites) is illustrated in Scheme I. In the first step, an *N*-acyl-2'-deoxynucleoside reacts with 1-(2-nitro-4,5-methylenedioxyphenyl)ethyl-1-chloroformate to yield 5'-MeNPoc-*N*-acyl-2'-deoxynucleoside. In the second step, the 3'-hydroxyl reacts with 2-cyanoethyl *N,N'*-diisopropylchlorophosphoramidite using standard procedures to yield the 5'-MeNPoc-*N*-acyl-2'-deoxynucleoside-3'-*O*-(2-cyanoethyl-*N,N'*-diisopropyl)phosphoramidites. The photoprotecting group is stable under ordinary phosphoramidite synthesis con-

ditions and can be removed with aqueous base. These reagents can be stored for long periods under argon at 4°C.

A 0.1 mM solution of each of the four deoxynucleosides—MeNPoc-dT, MeNPoc-dC<sup>ibu</sup>, MeNPoc-dG<sup>PAC</sup>, and MeNPoc-dA<sup>PAC</sup>—was prepared in dioxane. Aliquots (200  $\mu$ l) were irradiated with 14.5 mW of 365-nm light per cm<sup>2</sup> in a narrow-path (2 mm) quartz cuvette for various times. Four or five time points were collected for each base, and the solutions were analyzed for loss of starting material at 280 nm on a Nucleosil 5-C<sub>8</sub> HPLC column using a mobile phase of 60% (vol/vol) in water containing 0.1% (vol/vol) trifluoroacetic acid [MeNPoc-dT required a mobile phase of 70% (vol/vol) methanol in water]. Peak areas of the residual MeNPoc-*N*-acyl-deoxynucleoside were calculated, yielding photolysis half-times of 28 s, 31 s, 27 s, and 18 s for MeNPoc-dT, MeNPoc-dC<sup>ibu</sup>, MeNPoc-dG<sup>PAC</sup>, and MeNPoc-dA<sup>PAC</sup>, respectively. In all subsequent lithographic experiments, illumination times of 4.5 min ( $9 \times t_{1/2}$  MeNPoc-dC) were used to ensure >99% removal of MeNPoc protecting groups.

The synthesis support consists of a 5.1  $\times$  7.6 cm glass substrate prepared by cleaning in concentrated NaOH, followed by exhaustive rinsing in water. The surfaces were then derivatized for 2 hr with a solution of 10% (vol/vol) bis(2-hydroxyethyl)aminopropyltriethoxysilane (Petrarch Chemicals, Bristol, PA) in 95% ethanol, rinsed thoroughly with ethanol and ether, dried *in vacuo* at 40°C, and heated at 100°C for 15 min. In these studies, a synthesis linker is attached by reacting derivatized substrates with 4,4'-dimethoxytrityl (DMT)-hexaethyloxy-*O*-cyanoethyl phosphoramidite.



Scheme I

In a light-directed synthesis, the overall synthesis yield depends on the photodeprotection yield, the photodeprotection contrast, and the chemical coupling efficiency. Photo-kinetic conditions are chosen to ensure that photodeprotection yields are >99%. Unwanted photolysis in normally dark regions of the substrate can adversely affect the synthesis fidelity and can be minimized by using lithographic masks with a high optical density (5 OD units) and by careful index matching of the optical surfaces.

Two different methods were developed to investigate the chemical coupling efficiencies of the photoprotected nucleosides. First, the efficiencies were measured on hexaethylene glycol derivatized control pore glass. The glycol linker was detritylated and a MeNPoc-deoxynucleoside-*O*-cyanoethyl phosphoramidite coupled to the resin. Next, a DMT-deoxynucleoside-cyanoethyl phosphoramidite (reporter amidite) was added. The reporter amidite should couple to any unreacted hydroxyl groups remaining from the first coupling reaction. Following DMT deprotection, the trityl effluents were collected and quantified by absorption spectroscopy. In this assay, the coupling efficiencies are measured assuming a high coupling efficiency of the reporter amidite. The efficiencies of the MeNPoc-deoxyribonucleoside-*O*-cyanoethyl phosphoramidites to the hexaethylene glycol linker and the 16 different dinucleotide efficiencies were measured. The values ranged between 95% and 100% in this assay and were indistinguishable from values obtained with standard DMT-deoxynucleoside phosphoramidites.

To measure the coupling efficiency of the photoprotected nucleosides directly on the glass synthesis supports, each of the four MeNPoc-amidites was coupled to a substrate. A section of the substrate was deprotected by illumination and allowed to react against a MeNPoc-phosphoramidite. A new region of the substrate was then illuminated, a fluorescent deoxynucleoside phosphoramidite (FAM-phosphoramidite; Applied Biosystems) was coupled, and the substrate was scanned for fluorescence signal. Assuming that the fluorescently labeled phosphoramidite reacts at both the newly exposed hydroxyl groups and the previously unreacted hydroxyl groups, then the ratio of fluorescence intensities between the two sites provides a measure of the coupling efficiency. This measurement of the surface chemical coupling yields efficiencies ranging between 85% and 98%.

## RESULTS

**Spatially Directed Synthesis of an Oligonucleotide Probe.** To initiate the synthesis of an oligonucleotide probe, MeNPoc-dC<sup>ibu</sup>-3'-*O*-phosphoramidite was attached to a synthesis support through a linker (hexaethyloxy-*O*-cyanoethyl phosphoramidite). Regions of the support were activated for synthesis by illumination through 800 × 12800 μm apertures of a photolithographic mask. Seven additional phosphoramidite synthesis cycles were performed (with DMT-protected deoxynucleosides) to generate the sequence 3'-CGCATCCG. Following removal of the phosphate and exocyclic amine protecting groups with concentrated NH<sub>4</sub>OH for 4 hr, the substrate was mounted in a water-jacketed thermostatically controlled hybridization chamber.

**Hybridization of Targets to Surface Oligonucleotides.** To explore the availability of the support-bound octanucleotide probes for hybridization, 10 nM 5'-GCGTAGGC-fluorescein was introduced into the hybridization chamber and allowed to incubate for 15 min at 15°C. The surface was then interrogated with an epifluorescence microscope (488-nm argon ion excitation). The fluorescence image of this scan is shown in Fig. 2. The fluorescence intensity coincides with the 800 × 12800 μm stripe used to direct the synthesis of the probe. Furthermore, the signal intensities are high (four times over

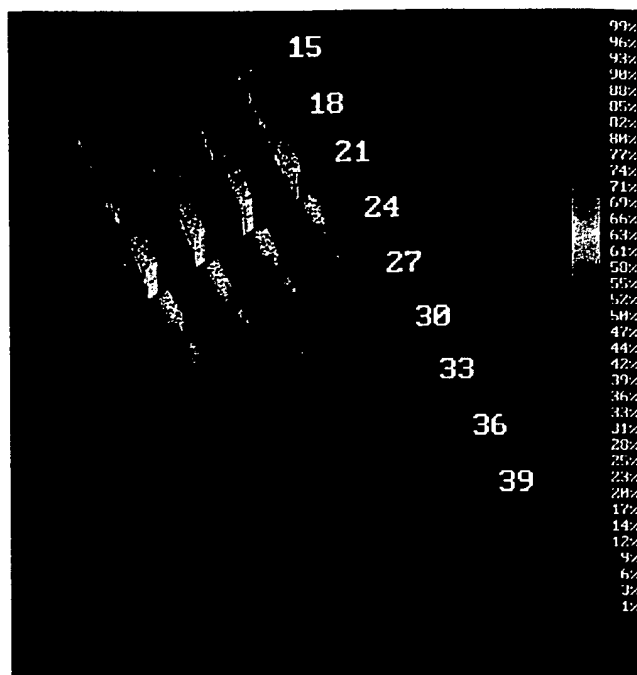


FIG. 2. Hybridization and thermal dissociation of oligonucleotides. Fluorescence scan of 5'-GCGTAGGC-fluorescein hybridized to complementary probes. The substrate surface was scanned with a Zeiss Axioscop 20 microscope using 488-nm argon ion laser excitation. The fluorescence emission above 520 nm was detected using a cooled photomultiplier (Hamamatsu 934-02) operated in photon-counting mode. The signal intensity is indicated on the color scale shown to the right of the image. The temperature is indicated to the right of each panel in °C.

the background of the glass substrate), demonstrating specific binding of the target to the probe.

The melting behavior of the target-probe complex was investigated by increasing the temperature in the hybridization chamber. After 10 min of incubation at each temperature, no significant changes in the fluorescence were observed, and the fluorescence intensities were recorded. The duplex melted in the temperature range expected for the sequence under study. The probes were stable to temperature denaturation of the target-probe complex as demonstrated by rehybridization of target DNA.

**Sequence Specificity of Target Hybridization.** To demonstrate the sequence specificity of probe hybridization, two different sequences were synthesized in 800 × 12800 μm stripes. Fig. 3A identifies the location of the two probes. The probe 3'-CGCATCCG was synthesized in stripes 1, 3, and 5. The probe 3'-CGCTTCCG was synthesized in stripes 2, 4, and 6. Fig. 3B shows the results of hybridizing 5'-GCGTAGGC-fluorescein to the substrate at 15°C. Although the probes differ by only one internal base, the target hybridizes specifically to its complementary sequence (~500 counts above background in stripes 1, 3, and 5) with little or no detectable signal in positions 2, 4, and 6 (~10 counts). Fig. 3C shows the results of hybridization with targets to both sequences. The signal in all positions in Fig. 3C illustrates that the absence of signal in Fig. 3B is due solely to the instability of the single base hybridization mismatch. Although the targets are present in equimolar concentrations, the ratios of signals in stripes 2, 4, and 6 in Fig. 3B are approximately 1.6 times higher than the ratios of signals in regions 1, 3, and 5, presumably due to slight differences in melting temperature values for the two duplexes. The duplexes were dissociated by raising the temperature to 45°C for 15 min, and the hybridizations were repeated in the reverse

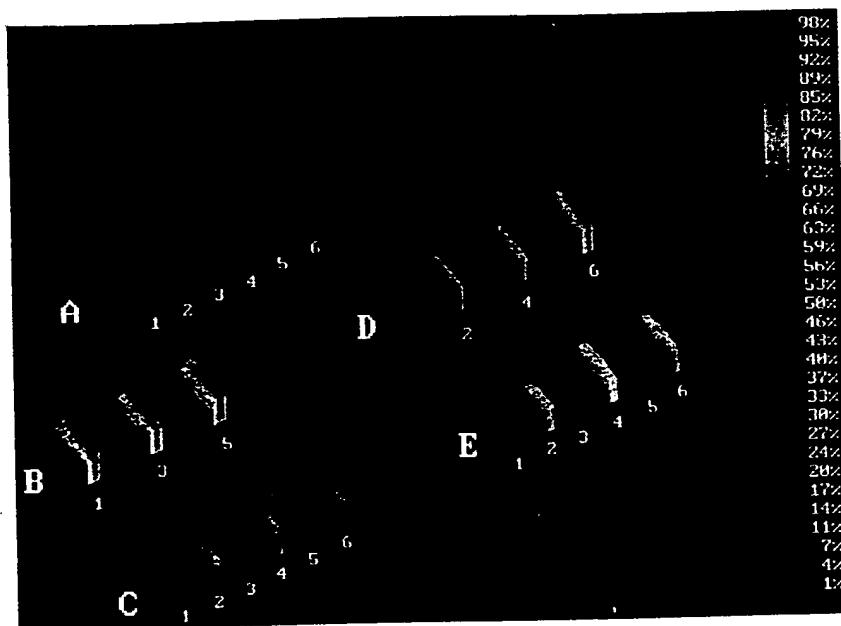


FIG. 3. Sequence specificity of hybridization. (A) Index of the probe composition at each synthesis site. 3'-CGCATCCG was synthesized in stripes 1, 3, and 5, and 3'-CGCTTCCG was synthesized in stripes 2, 4, 6. (B) Fluorescence image showing hybridization of substrate with 10 nM 5'-GCGTAGGC-fluorescein. Hybridization was performed in 6× SSPE (1 M NaCl/66 mM sodium phosphate/6 mM EDTA, pH 7.4)/0.1% Triton X-100 at 15°C for 15 min. (C) Hybridization with 10 nM 3'-GCGAAGGC added to the hybridization solution of B. (D) After high-temperature dissociation of fluoresceinated targets from C, the substrate was incubated with 10 nM 3'-GCGAAGGC at 15°C for 15 min. (E) Hybridization with 10 nM 3'-GCGTAGGC added to the hybridization solution of D.

order (Fig. 3 D and E), demonstrating specificity of hybridization in the reverse direction.

**Combinatorial Synthesis of a Probe Matrix.** In a light-directed synthesis, the location and composition of products depend on the pattern of illumination and the order of chemical coupling reagents (6). Consider the synthesis of 256 tetranucleotides, as illustrated in Fig. 4. Mask 1 activates one-fourth of the substrate surface for coupling with the first of 4 nucleosides in the first round of synthesis. In cycle 2, mask 2 activates a different quarter of the substrate for coupling with the second nucleoside. The process is continued to build four regions of mononucleotides. The masks of round 2 are perpendicular to those of round 1, and each cycle generates four new dinucleotides. The process continues through round 2 to form 16 dinucleotides as illustrated in Fig. 4. The masks of round 3 further subdivide the synthesis regions so that each coupling cycle generates 16 trimers. The subdivision of the substrate is continued through round 4 to form the tetranucleotides. The synthesis of this probe matrix can be compactly represented in polynomial notation (6) as  $(A + C + G + T)^4$ . Expansion of this reaction polynomial identifies the 256 tetranucleotides.

The potential of light-directed combinatorial synthesis can be appreciated by the combinatorial synthesis of the probe matrix shown in Fig. 5A. The polynomial for this synthesis is given by  $3'-CG(A + G + C + T)^4CG$ . The synthesis map is given in Fig. 5B. All possible tetranucleotides are synthesized flanked by CG at the 3' and 5' ends. Hybridization of the target 5'-GCGGCGGC-fluorescein to this array at 15°C yields

the 3'-CGCCGCCG complementary probe as the most intense position (2698 counts). Significant intensity is also observed for the following mismatches: 3'-CGCAGCCG (554 counts), 3'-CGCCGACG (317 counts), 3'-CGCCGTCG (272 counts), 3'-CGACGCCG (242 counts), 3'-CGTCGCCG (203 counts), 3'-CGCCGCCG (180 counts), 3'-CGCTGCCG (163 counts), 3'-CGCCACCG (125 counts), and 3'-CGCCTCCG (78 counts).

## DISCUSSION

Arrays of oligonucleotides can be efficiently generated by light-directed synthesis and can be used to determine the identity of DNA target sequences. As shown here, an array of all tetranucleotides was produced in 16 cycles requiring 4 hr to complete. Because combinatorial strategies are used (6), the number of compounds increases exponentially while the number of chemical coupling cycles increases only linearly. For example, expanding the synthesis to the complete set of  $4^8$  (65,536) octanucleotides will add only 4 hr to the synthesis for the 16 additional cycles. Furthermore, combinatorial synthesis strategies can be implemented to generate arrays of any desired composition (6). For example, since the entire set of dodecamers ( $4^{12}$ ) can be produced in 48 photolysis and coupling cycles ( $b^n$  compounds requires  $b \times n$  cycles), any subset of the dodecamers (including any subset of shorter oligonucleotides) can be constructed with the correct lithographic mask design (6) in 48 or fewer chemical coupling steps. The number of compounds in an array is limited only

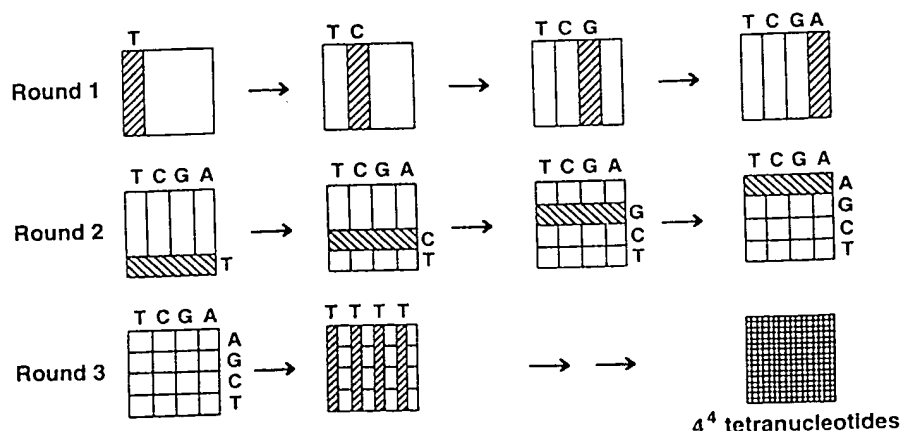


FIG. 4. Combinatorial synthesis of  $4^4$  tetranucleotides. In round 1, one-fourth of the synthesis area is activated by illumination through mask 1 for coupling of the first MeNPoc-nucleoside (A in this case). In cycle 2 of round 1, mask 2 activates a different one-quarter section of the synthesis substrate and a different nucleoside (T) is coupled. Further lithographic subdivisions of the array and chemical couplings generate the complete set of 256 tetranucleotides as described in the text.

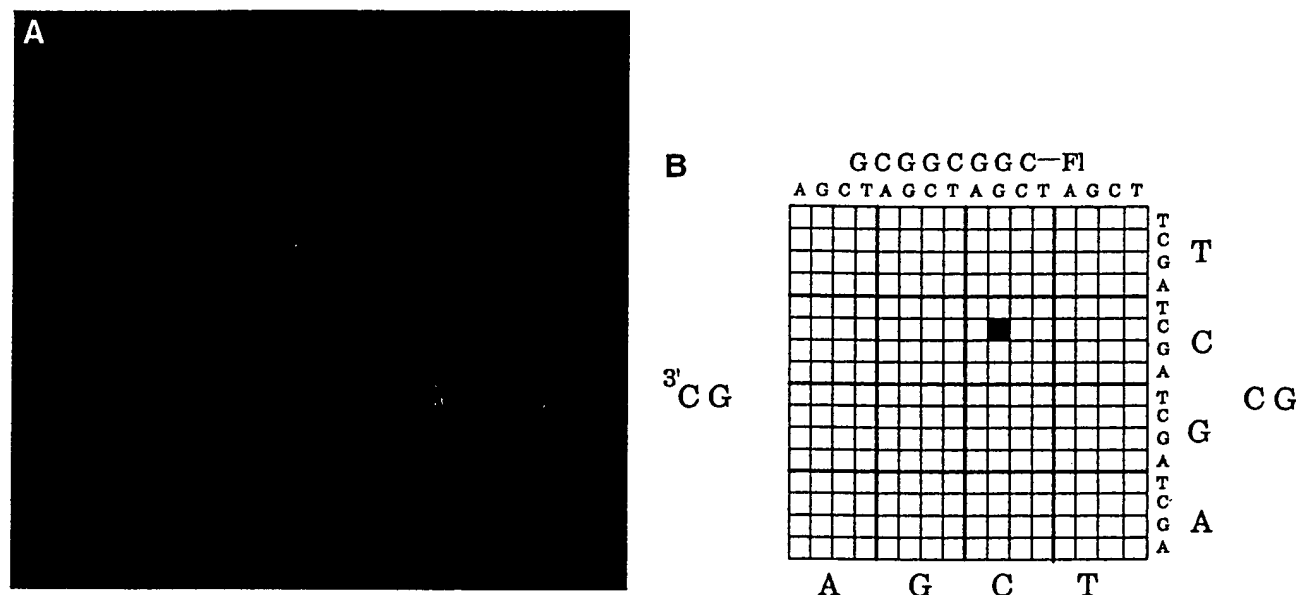


FIG. 5. Hybridization to a matrix of 256 octanucleotides. (A) Fluorescence image of a 256-octanucleotide array following hybridization with 10 nM 5'-GCGGCGGC-fluorescein in  $6\times$  SSPE/0.1% Triton X-100 for 15 min at 15°C. (B) Matrix decoder for the array. The matrix synthesis is represented by the polynomial  $3'\text{-CG}(\text{A} + \text{G} + \text{C} + \text{T})^4\text{CG}$ . The site containing the complementary sequence 3'-CGCGCCCG is highlighted for reference.

by the density of synthesis sites and the overall array size. Recent experiments have demonstrated hybridization to probes synthesized in 25- $\mu\text{m}$  sites. At this resolution, the entire set of 65,536 octanucleotides can be placed in an array measuring 0.64-cm square, and the set of 1,048,576 dodecanucleotides requires only a 2.56-cm array.

Genome sequencing projects will ultimately be limited by DNA sequencing technologies. Current sequencing methodologies are highly reliant on complex procedures and require substantial manual effort (8, 9). SBH has the potential for transforming many of the manual efforts into more efficient and automated formats. Light-directed synthesis is an efficient means for enabling SBH and for the large-scale production of miniaturized arrays.

Oligonucleotide arrays are not limited to primary sequencing applications. Because single base changes cause multiple changes in the hybridization pattern, the oligonucleotide arrays will provide a powerful means to check the accuracy of previously elucidated DNA sequence or to scan for changes within a sequence. In the case of octanucleotides, a single base change in the target DNA results in the loss of eight complements and generates eight new complements. Matching of hybridization patterns may be useful in resolving sequencing ambiguities from standard gel techniques or for rapidly detecting DNA mutational events.

The potentially very high information content of light-directed oligonucleotide arrays will change genetic diagnostic testing. Sequence comparisons of hundreds to thousands of different genes will be assayed simultaneously instead of the current one, or few at a time format. Custom arrays can also be constructed to contain genetic markers for the rapid identification of a wide variety of pathogenic organisms.

Oligonucleotide arrays can also be applied to study the sequence specificity of RNA- or protein-DNA interactions. Experiments can be designed to elucidate specificity rules of non-Watson-Crick oligonucleotide structures or to investigate the use of novel synthetic nucleoside analogs for antisense or triple helix applications. Suitably protected RNA monomers may be employed for RNA synthesis. The oligonucleotide arrays should find broad application deducing the thermodynamic and kinetic rules governing formation and stability of oligonucleotide complexes.

We are grateful to L. Stryer, P. Schultz, and F. Pease for their critical reading and helpful comments on the manuscript. A.C.P. is a National Institutes of Health postdoctoral fellow (HG 00060). This work was sponsored in part by National Institutes of Health (HG 00813) and Department of Energy (DE FG03 92ER) grants to S.P.A.F.

1. Lysov, Yu. P., Florentiev, V. L., Khorlyn, A. A., Khrapko, K. R., Shick, V. V. & Mirzabekov, A. D. (1988) *Dokl. Akad. Nauk SSSR* 303, 1508-1511.
2. Bains, W. & Smith, G. C. (1988) *J. Theor. Biol.* 135, 303-307.
3. Drmanac, R., Labat, I., Brukner, I. & Crkvenjakov, R. (1989) *Genomics* 4, 114-128.
4. Strezoska, Z., Paunesku, T., Radosavljevic, D., Labat, I., Drmanac, R. & Crkvenjakov, R. (1991) *Proc. Natl. Acad. Sci. USA* 88, 10089-10093.
5. Drmanac, R., Drmanac, S., Strezoska, Z., Paunesku, T., Labat, I., Zeremski, M., Snoddy, J., Funhkhouer, W. K., Koop, P., Hood, L. & Crkvenjakov, R. (1993) *Science* 260, 1649-1652.
6. Fodor, S. P. A., Read, J. L., Pirrung, M. C., Stryer, L., Tsai Lu, A. & Solas, D. (1991) *Science* 251, 767-773.
7. Southern, E. M., Maskos, U. & Elder, J. K. (1992) *Genomics* 13, 1008-1017.
8. Sanger, F., Nicklen, S. & Coulson, A. R. (1977) *Proc. Natl. Acad. Sci. USA* 74, 5463-5467.
9. Maxam, A. M. & Gilbert, W. (1977) *Proc. Natl. Acad. Sci. USA* 74, 560-564.

Q  
11  
N26  
v. 91  
no. 11  
BIOS  
Campus

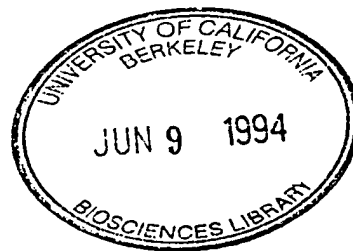
MAY 24, 1994

VOLUME 91

NUMBER 11



# Proceedings OF THE National Academy of Sciences



OF THE UNITED STATES OF AMERICA

The Library - UC Berkeley  
Received on: 06-10-94  
Proceedings of the National  
Academy of Sciences of the  
United States of America  
UNTIL

JUN 40 1994



## Contents

Specific association between the human DNA repair proteins XPA and ERCC1 Lei Li, Stephen J. Elledge, Carolyn A. Peterson, Elise S. Bales, and Randy J. Legerski	5012-5016	Current rectification of an uncharged peptide ion channel Paul K. Kienker, William F. DeGrado, and James D. Lear	4859-4863
Formation of a ternary complex by human XPA, ERCC1, and ERCC4(XPF) excision repair proteins Chi-Hyun Park and Aziz Sancar	5017-5021	Direct determination of layer packing for a phospholipid solid solution at 0.32-nm resolution Douglas L. Dorset	4920-4924
Light-generated oligonucleotide arrays for rapid DNA sequence analysis Ann Caviani Pease, Dennis Solas, Edward J. Sullivan, Maureen T. Cronin, Christopher P. Holmes, and Stephen P. A. Fodor	5022-5026	An algorithm to generate low-resolution protein tertiary structures from knowledge of secondary structure Alessandro Monge, Richard A. Friesner, and Barry Honig	5027-5029
Molecular interactions between interferon consensus sequence binding protein and members of the interferon regulatory factor family Chiara Bovolenta, Paul H. Driggers, Michael S. Marks, Jeffrey A. Medin, Alexander D. Politis, Stefanie N. Vogel, David E. Levy, Kazuyasu Sakaguchi, Ettore Appella, John E. Coligan, and Keiko Ozato	5046-5050		
Molecular cloning of the gene encoding the mouse parathyroid hormone/parathyroid hormone-related peptide receptor Kimberly A. McCuaig, John C. Clarke, and John H. White	5051-5055		
Qualitative changes in the subunit composition of $\kappa$ B-binding complexes during murine B-cell differentiation Shigeki Miyamoto, Mark J. Schmitt, and Inder M. Verma	5056-5060		
Solution NMR structure of the major cold shock protein (CspA) from <i>Escherichia coli</i> : Identification of a binding epitope for DNA Keith Newkirk, Wenqing Feng, Weining Jiang, Roberto Tejero, S. Donald Emerson, Masayori Inouye, and Gaetano T. Montelione	5114-5118		
Crystal structure of CspA, the major cold shock protein of <i>Escherichia coli</i> Hermann Schindelin, Weining Jiang, Masayori Inouye, and Udo Heinemann	5119-5123		
Three-dimensional working model of M1 RNA, the catalytic RNA subunit of ribonuclease P from <i>Escherichia coli</i> Eric Westhof and Sidney Altman	5133-5137		
Chemical synthesis of a fully active transcriptional repressor protein Gloria del Solar, Fernando Albericio, Ramón Eritja, and Manuel Espinosa	5178-5182		
X-ray structure of a cyclophilin B/cyclosporin complex: Comparison with cyclophilin A and delineation of its calcineurin-binding domain Vincent Mikol, Jörg Kallen, and Malcolm D. Walkinshaw	5183-5186		
<b>BIOPHYSICS</b>		<b>CELL BIOLOGY</b>	
Inversion of the Bohr effect upon oxygen binding to 24-meric tarantula hemocyanin Reinhard Sterner and Heinz Decker	4835-4839	Adipocyte differentiation selectively represses the serum inducibility of <i>c-jun</i> and <i>junB</i> by reversible transcription-dependent mechanisms Hanlin Wang and Robert E. Scott	4649-4653
		Unidirectional fluxes of rhodamine 123 in multidrug-resistant cells: Evidence against direct drug extrusion from the plasma membrane Guillermo A. Altenberg, Carlos G. Vanoye, Julie K. Horton, and L. Reuss	4654-4657
		Invasiveness and metastasis of NIH 3T3 cells induced by Met-hepatocyte growth factor/scatter factor autocrine stimulation Sing Rong, Shraga Segal, Miriam Anver, James H. Resau, and George F. Vande Woude	4731-4735
		Molecular cloning, tissue distribution, and expression of a 14-kDa bile acid-binding protein from rat ileal cytosol Yong-Zhong Gong, Eric T. Everett, David A. Schwartz, James S. Norris, and Frederick A. Wilson	4741-4745
		Mitogen-stimulated phosphorylation of histone H3 is targeted to a small hyperacetylation-sensitive fraction Michael J. Barratt, Catherine A. Hazzalin, Eva Cano, and Louis C. Mahadevan	4781-4785
		Rat liver endocytic coated vesicles do not exhibit ATP-dependent acidification <i>in vitro</i> Renate Fuchs, Adi Ellinger, Margit Pavelka, Ira Mellman, and Herbert Klapper	4811-4815
		A G protein-coupled receptor with low density lipoprotein-binding motifs suggests a role for lipoproteins in G-linked signal transduction Cornelis P. Tensen, Ellen R. van Kesteren, Rudi J. Planta, Kingsley J. A. Cox, Julian F. Burke, Harm van Heerikhuizen, and Erno Vreugdenhil	4816-4820
		Posttranscriptional mRNA processing as a mechanism for regulation of human A <sub>1</sub> adenosine receptor expression Hongzu Ren and Gary L. Stiles	4864-4866
		Mammalian mitogen-activated protein kinase kinase (MEKK) can function in a yeast mitogen-activated protein kinase pathway downstream of protein kinase C Kendall J. Blumer, Gary L. Johnson, and Carol A. Lange-Carter	4925-4929